UDC 621.9.011:517.962.1

FEA-AUDIT AND LOCAL REDESIGN OF PRACTICE-PROVED LABORATORY CENTRIFUGE MACHINE

[1]Dounar S., [1]Iakimovitch A., [1]Shirvel P., [2]Jakubowski A., [2]Chybowski L., [3]Tanishq J. M., [1]Penkina A.

[1]Belarusian National Technical University, Minsk, Belarus
[2]Maritime University of Szczecin, Szczecin, Poland
[3]AcculightUSA, Elk Grove Village, U.S.A

Centrifuge is a good knew type of machines for liquid separation [1]. Given work touches the compact, high-speed biological centrifugal machine, designed before FEA [2] epoch, but permanently produced and exploited till now. So some kind of FEA-audit of old, intuitive design is provided here. FEA-simulation was based on the experience gained at rotating technological machines [3–5].

Proportions of centrifuge *load-bearing system* (LBS) are optimized and proved by long-term practice (more than 20 years of production, first examples are still in service). The system was designed a long time ago, but collapses and partial cracking are not reported for all centrifuges.

Centrifuge refers to the reliable swing-bucket type of rotor [6]. It works in the quasi-static mode with long time loading by constant centrifugal forces caused by stable rotation at the speed $N_c = 4000\ \text{min}^{-1}$. Quantity of loading cycles (due to speeding up and running out) is not large for all service life. So static strength and, possibly, ratcheting [7] (accumulation of plastic deformation in the stress concentrators during low-cycle fatigue) are the main issues.

Technological limitations exert minimal influence on the design. All structural parts for years are machined at the 5-axis CNC machine tools. Only high-grade materials in the monolithic form are used for structural parts machining. Shakedown procedure during very first rotation is accomplished for all centrifuges. Solid weight is used instead of envelope with the liquid to process. It caused 15 % increasing of centrifugal forces. All centrifuges steady survives shakedown with no faults.

Shakedown of any LBS make sense while local plastic deformations are expected in the stress concentrators [8]. It creates residual stresses preventing further plastic deformation at the next load cycles. Such reinforcing effect is known as autofrettage [9]. In case of excessive cycle loading places of autofrettage became the ratcheting spots. It leads to low-cycle fatigue fracture.

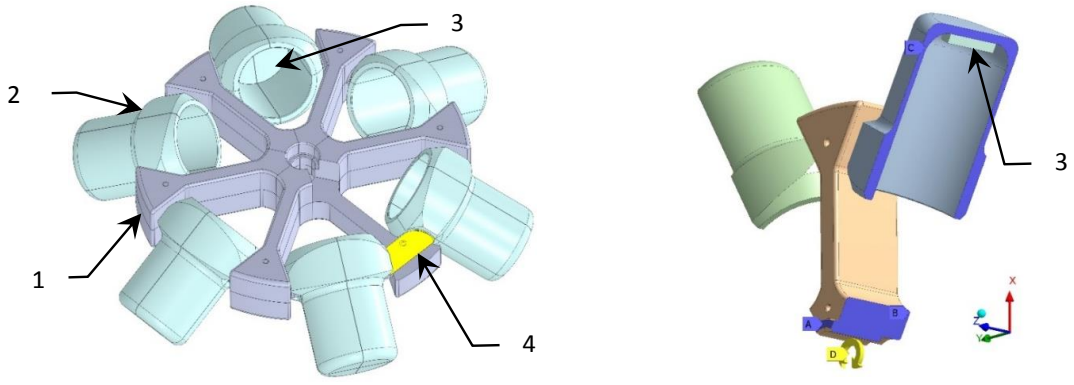

a) *b)*

Fig. 1. Rotated load-bearing system (LBS) of the centrifuge (a) and symmetrical 1/6-part of the model (b): 1 – rotor; 2 – bucket; 3 – weight; 4 – pin. A, B, C – slick unmovable rests; D – angular velocity applying

Some specific terms are proposed in that work here below:

Critical point of surviving (CPS) – severe stress concentrator possesses features: a) almost inevitable in the design sense; b) haven't got a reservation if cracked; c) shortage of effective parameters to control the level of stress in it. CPS are tied to different inner corners and fillets.

Fillet radius management (FRM) – need to vary fillet radius for CPS smoothing, causing no indirect damages and harmful consequences for nearby design.

Contact spot control (CSC) – design approach aiming to reduce nominal contact interface to dimensions of expected virtual contact spot. It gives room for e. g. CPS smoothing.

Fig.1, a gives an outer view of the centrifuge's load-bearing system (LBS). Fig. 1, *b* depicts 1/6 portion of the full symmetrical model. The section view on the rotating structural parts is given in fig. 2. The set of parts consists of the aluminum rotor 1 (outer diameter ø205 mm; six spokes 1S protruded radially from the hub 1H) and six aluminum buckets 2 (height 162 mm), containing processed liquids in the flexible envelopes (not showed). In that work envelopes are replaced by weights 3, secured to the bucket bottoms. There is lug 1L at the end of each spoke. Lug holds pin 4.

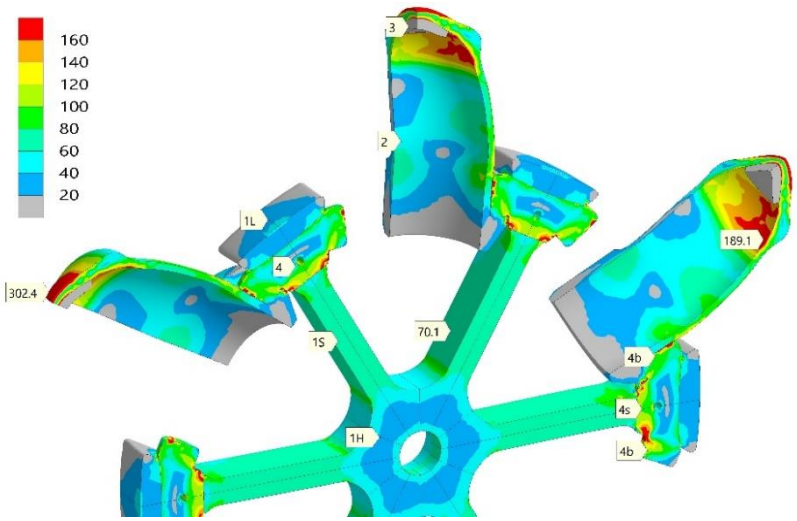

Fig. 2. Section view of the symmetrical ½-part of the model with the distribution of the equivalent stresses σ_e (MPa), caused by angular velocity $\omega = 420$ rad/s. Only quarters of buckets 2 and weights 3 are shown. Marks 1L, 1S, 1H relate to the rotor 1; marks 4b, 4s – to the pin 4. EL, BC

Two neighboring pins 4 hold the bucket 2 between spokes with the possibility of local rocking. Every pin possesses three cylindrical steps. The central step of ø32 mm (call it – stem – 4S) is inserted into spoke lug (1L) and fixed. End steps (bosses – 4B; ø30 mm) stay in frictional contact with buckets 2. Axes of the bosses inclined at 30 degrees to the axis of the stem in the rotational plane (fig. 3).

That work conservatively describes just shakedown procedure, where instead of envelope the weights 3 of the same mass (0.9 kg) is simulated.

FE model building was provided focusing on the surface layers precise meshing. The critical region of centrifugal LBS is the pin with mating them rotor lug and bucket slot (fig., 3 *a, b*). Axes of the pin stem St and pin boss B are inclined to each other at 30º. So special shoulder Sh is necessary. Shoulder conjugates with boss by fillet F. Current (existing) fillet radius is stated by drafts as $r_f \leq 1$ mm. That design will be referenced below as ***Des1***.

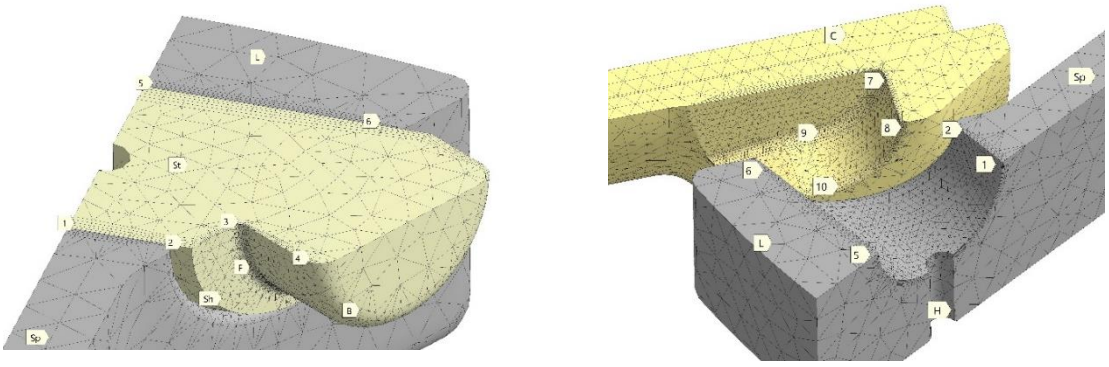

a) *b)*

Fig. 3. Geometry and mesh for pin and mating parts: bucket slot C showed only (*b*); pin (stem St plus boss B is visible (*a*)

Contact surface 1-2-6-5 is shown as the lug L hole in fig.3, b. Small hole H is aimed at the pin fixation. There is slot in the bucket L (fig. 3, *b*). It's surface 7–8–9–10 mates with the pin boss. Both parts are pressed to each other by centrifugal forces. Bucket slot is paved by 5 thin FE layers. Lug and rotor spoke Sp is simulated by the common mesh with relatively rare meshing of inner volumes.

Pin is made from hardened stainless steel 14X17H2 (GOST analog of AISI 431; yield stress $\sigma_y = 810$ MPa). Rotor and buckets are from the aluminum alloy B95 (yield stress 420 MPa).

Allowable stresses may be taken from respectable German standard DIN 15018, dealing with technological machine strength. Static (and quasi-static) loading needs working stresses σ_{th} to be lower than yield stress σ_y according to formula $\sigma_{th} \leq \sigma_y/1.5$. It touches spacy stresses (frequently called *nominal stresses*). Appropriated level of local stresses into concentrators is not too evident.

The task is treated as fully static. Only centrifugal forces are applied by rotational velocity $\omega = 420\ \mathrm{s}^{-1}$. Speeding-up nor run-out is simulated. The geometrical model is taken as fully symmetrical. Only 1/24 – part of the model is sufficient to represent a situation. Constraint conditions are represented only by slippy rests due to only symmetrical parts of model were modelled.

The simulation was provided for a bunch of models and variants. Survey (introducing) variants are fully linear, elastic (*EL*), with one-step loading. All contact pairs in that cases were switched to the bonded status (*BC*). Final simulations included an accounting of geometry non-linearities (always), plastic deformation (mark it *PL*), and frictional contact effects (*FC*). A standard small-step loading procedure was provided. Technic of "weak springs" is used to insure convergence of iteration procedure at very beginning of loading.

All frictional contact pairs were initially adjusted to touch, without inner gaps or pre-stress. Friction coefficient $\mu = 0.2$ was appointed for all pairs. Contact sliding was tracked during loading. Sliding distance was not exceed several dozen of micrometers. Contact spot changes were noticed.

Contact force reaches 43.3 kN at the every pin boss. It is causes by centrifugal forces applied to the weight (0.9 kg) and to the bucket (1.24 kg). Contact forces evoke radial tension inside every rotor spoke. However rotor strength is quite sufficient in general. Fig. 2 shows according picture of the equivalent stress σ_e for the linear model with bonded contact pairs.

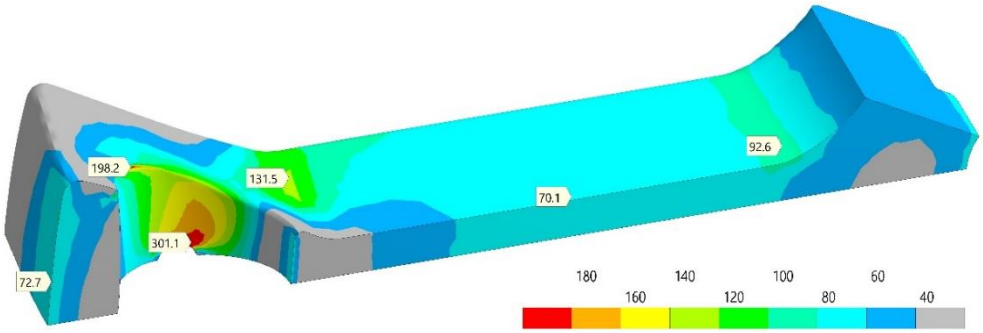

Fig. 4. Distribution of the equivalent stresses σ_e (MPa) in the rotor spoke with adjacent lug (at the left) and hub (at the right) (one-quarter model; FC, EL). Angular velocity $\omega = 420\,\mathrm{rad/s}$;×50

All stresses are relatively low in the rotor. Every spoke (1S) undergoes moderate, near-uniform tension (mark 70.1 MPa). It is much lower, then assigned yield stress of the aluminum alloy (420 MPa). Stress concentrators in the centrifuge LBS are all tied to pins and to bottoms of buckets.

Fig. 4 depicts the distribution of σ_e in the rotor itself for simulation with friction contacts (FC). The situation is caused at whole by radial tension. Only slight stress concentration is revealed on the spoke-hub junction (92.6 MPa instead 70.1 MPa in the middle of spoke). Transient rounding between spoke and lug is stressed a little bit more – 131.5 MPa (concentration in 1.87 times). Attention should be paid to the edge of the pin-hole (198.2 MPa). However, really dangerous place is a small auxiliary hole (for pin fastening), where σ_e reaches 301.1 MPa. Such stress level is hardly approvable in comparison with yield stress $\sigma_y^{al} = 420$ MPa.

Centrifuge stresses accumulate mostly in the pin regions. Let's name (fig. 5, *a*) contact pair "pin – bucket" as interface ***CI-1*** (mark *463.5*), and contact pair "pin – rotor spoke" as ***CI-2*** (marks *214.2 – 16.6 – 0*). Contact interface ***CI-2*** is partially opened (mark 0) from the side of the centrifuge axis. Contact pressure concentrates on the edge of pin hole (mark *214.2*). Pressure is just low in the middle of the spoke lug (mark *16.6* at the fig. 5, *a* and mark *2* at the fig 5, *b*).

Contact interface ***CI-1*** is more stressful. Its feature is linear virtual contact (through mark *463.5* at the fig. 5, *a*). That line corresponds to the edge 1 (fig. 5, *a*) on the pin boss.

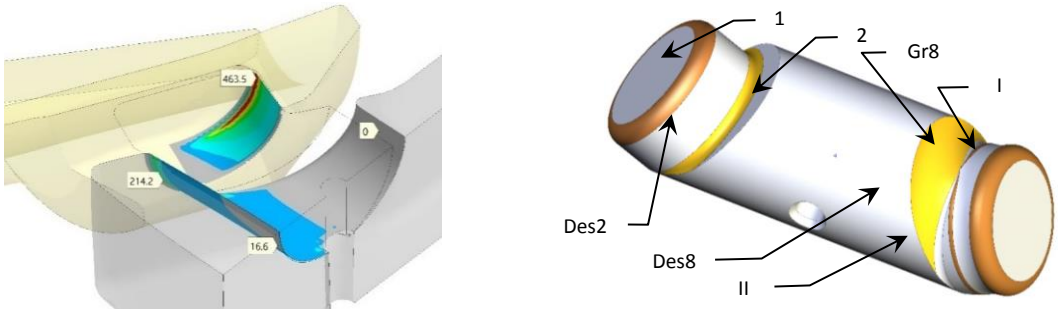

a) *b)*

Fig. 5. Compressing stresses (*a*) in the contacts "pin (shown separately on b) – bucket slot" (up to 463.5 MPa) and "pin stem – spoke lug" (up to 214.2 MPa). EL, FC

Linear-like contact ***CI-1*** reflects by narrow strips on the pictures of bucket stress state (fig. 6). Tension stress concentrator (mark 215.27) is visible (fig. 6, *a*) in the bucket slot on the σ_1 distribution. Strip of high compression (mark 332.65 on the fig. 6, *b*) is depicted on the σ_3 picture. The last strip precisely coincides with linear ***CI-1*** contact. Tension strip is place of centrifugal force collecting.

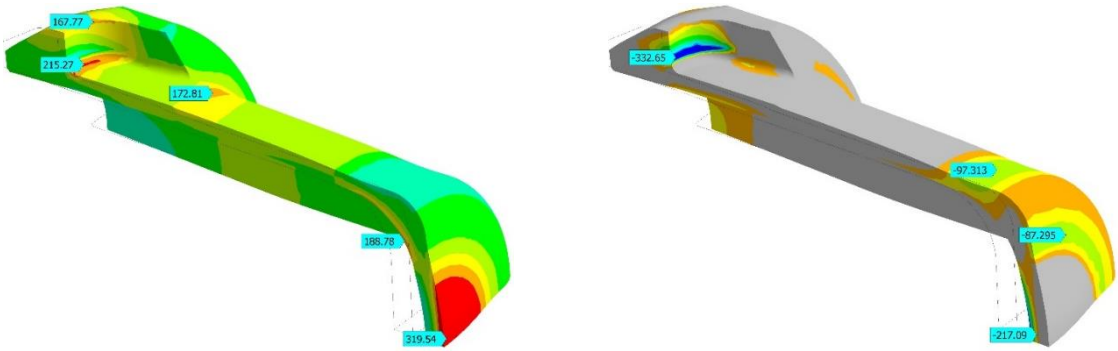

a) *b)*

Fig. 6. Stress state in the bucket (¼ part) during rotation with angular velocity $= 420\ \mathrm{rad/s}$: *a* – distribution of maximal principal stress σ_1; *b* – picture of the minimal stress σ_3 . EL, FC, MPa, ×20

Fig. 6 pointed out overstress of the bucket bottom. There are two regions of strong bending – at the center of the bottom (marks 319.54 – –217.09) and on the transition "bottom – shell" (marks 188.78 – –87.295). Surface plastic deformations are near to start at the bottom center.

The strongest stress concentration is revealed on the pin fillet F (fig. 3). Elastic solution for frictional contacts (fig. 7, *a*) shows equivalent stress (mark 1222) exceeding one and half times yield stress. Two-axial tension governs on the fillet surface ($\sigma_1 = 1351$ MPa, $\sigma_2 = 343M$ Pa, $\sigma_3 = 0$).

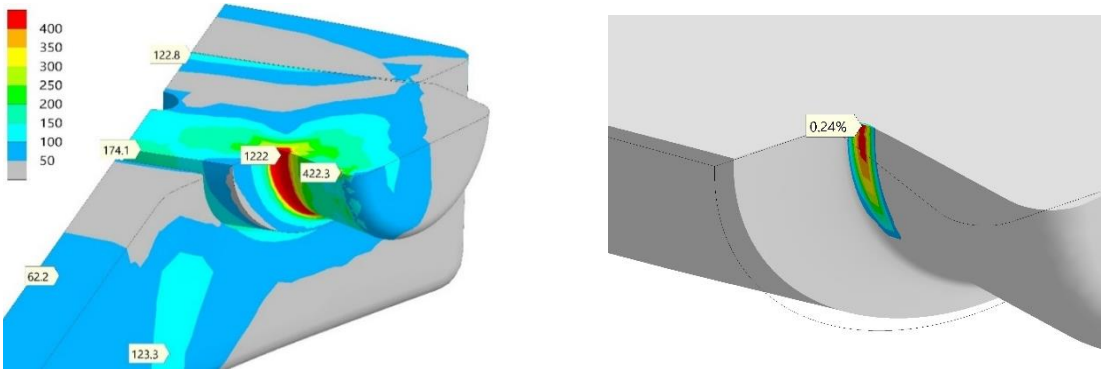

a) *b)*

Fig. 7. Distribution of the equivalent stresses σ_e (MPa) in the pin ($r_f \leq 1$mm) and rotor lug (a – EL, FC) and plastic deformation focus on the pin fillet surface (b – PL, FC). $\omega = 420\ \mathrm{rad/s}$; ×50

Elastic-plastic solution (fig. 7, *b*) reveals significant plastic deformation on the fillet (mark 0.25 %). It is unsafe situation due to preliminary steel hardening. Local plastic overloading of the hardened pin may leads to the brittle fracture.

Fillet F should be taken as a specific object – critical points of surviving – CPS. One could see strong imminent stress concentration, on the one hand. On the other hand, long service life of centrifugal machine gives evidence of material surviving into fillet region. It is possible, qualitative steel possesses durability resources even in the hardened state. Feasible issue may be autofrettage effect, when overloading causes plastic deformation and residual stresses. That stresses could envelope CPS and compensate partially working stresses. Plastic deformation of the hardened pin fillet points out at the uninvestigated marginal field of the steel strength. Looks like hardened steel is able to withstand some local plastic flow in the repeatable manner. Though condition and safety frames of such surviving are really unclear.

Discussion about optimization. Pin fillet CPS needs to be smoothed out. Full CPS excluding is hardly possible. It is caused by logic of the console beam (pin boss) loading. Hardness and ductility should be brought to the problem area at the same time [10]. Obviously, pin should be accomplished from functional gradient material (FGM) [11]. High hardness of surface layers would be sufficient to confine fillet region in the fully elastic conditions. However, FGM approach needs time, sustained pin production and cost. Nearby solutions are shot peening [12] and laser treatment [13] in the synergetic way.

Both technologies are effective for relatively opened features at the processed part. For example, blasted shot flow hardly reaches small rounds in the inner corners (discussed case). Thus, pin should be redesigned with more exposed fillet.

Filling the step between stem and boss at the pin was provided by *fillet radius management* (FRM) approach (fig. 3, *a*). Initial fillet F radius value $r_f = 1$ mm (***Des1***) was changed to the 2, 4, 8 mm (design variants Des2, Des4, Des8 respectively). It is necessary to find the room for Des4, Des8 solution. Technics CSC could do it by contact interface CI-1 decreasing (fig. 5, *b* – right end).

Double increasing of fillet radius lowers peak tension stress. Stress σ_1 decreases from 1351 MPa ($r_f = 1$ mm; fig. 7, *a*) to 883 MPa ($r_f = 2$ mm; fig. 8, *b*). Small plastic deformations $\varepsilon_{pl}^{ac} < 0.015$ are revealed on fillet. So larger radius relives danger of surface fracture.

CSC technics proposes (fig. 8, right pin ends) to increase fillet radius up to limit and exclude the pin step completely. Step would be overrode by complex surface Sm8. Radius 8 mm is achieved in the point C. Such overriding leads to the significant weakening of tension. Mark *470.99* points out moderate σ_1 stress. It is two times lower as for Des2 (left pin ends on fig. 8 – mark *883.27*). CSP is smoothed out. Possibility cracking becomes weak.

Room for larger fillet was found by shrinkage of "pin – bucket" contact spot (interface ***CI-1***). Initial cylindrical boss was ultimately overrode by fillet itself and groove Gr8 (fig. 8, *b*). That groove is shallow. Gr8 profile is incorporated inside smoothing arc CA (fig. 8, *a*). Groove Gr8 is the extension of the fillet and take part in the stress alleviation. Approach FRM collaborates here with CSC.

As for design Des8, pin can interacts with the bucket only along R3 toroidal surface (fig. 8, *c*), conjugated with Gr8 and having 3 mm radius. Mean R3 contact place as primary contact spot.

Ledge C4 may be optionally shaped on the pin boss. Here ledge is rounded by radius 4 mm. Possibility of free rotation is preserved for "pin – bucket" joint. Ledge C4 may be named as secondary contact spot. Both spots are clearly visible on the fig. 8, *c* (right side). Every pin end possess one primary spot and two secondary ones. It brings reliable three-point basing of bucket upon the pin.

Ultimate pin step smoothing brings the problem of high contact pressure (fig. 9). Standard shape of contact spot is visible on the left side of picture ($r_f = 2$ mm, Des2). Triangle spot with vertexes O-0, O-1 and O-2 shows moderate pressure concentration, slightly exceeded 300 MPa level.

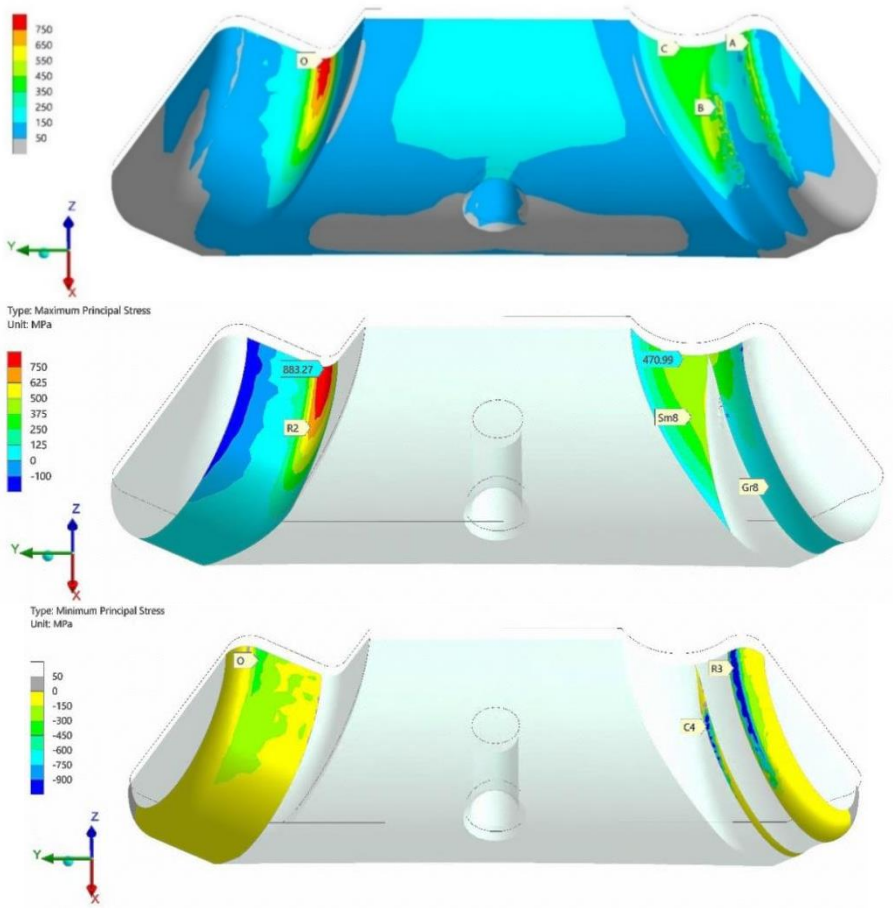

(a

(b

(c

Fig. 8. Design variants Des2 ($r_f = 2$ mm, left) and Des8 ($r_f = 8$ mm, right) for pin: *a* – picture of equivalent stress σ_e; *b* – distribution of maximal principal stress σ_1(tension); *c* – dispensation of minimal principal stress σ_3(compression). EL, FC, MPa; angular velocity $\omega = 420\,\mathrm{rad/s}$; ×15

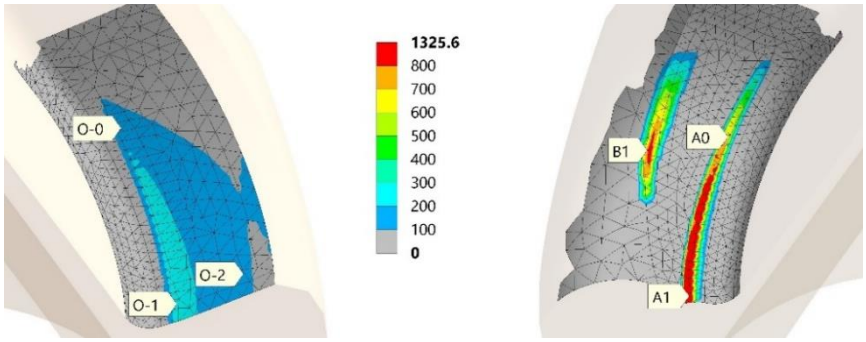

Fig. 9. Contact pressure (MPa) distribution in the bucket slot for Des2 (left) and Des8 (right) pin design variants (EL, FC). ×15

Pressure level increases threefold and more for 3-point basing according to Des8 variant (fig. 10, right, $r_f = 8\,mm$). Primary spot A0 – A1 and secondary one B1 are both clearly observable. Spot B1 bears about one third part of the full contact force. Small squares of spots may cause local plastic squeezing. Bucket contact surface should be treated e. g. by laser hardening.

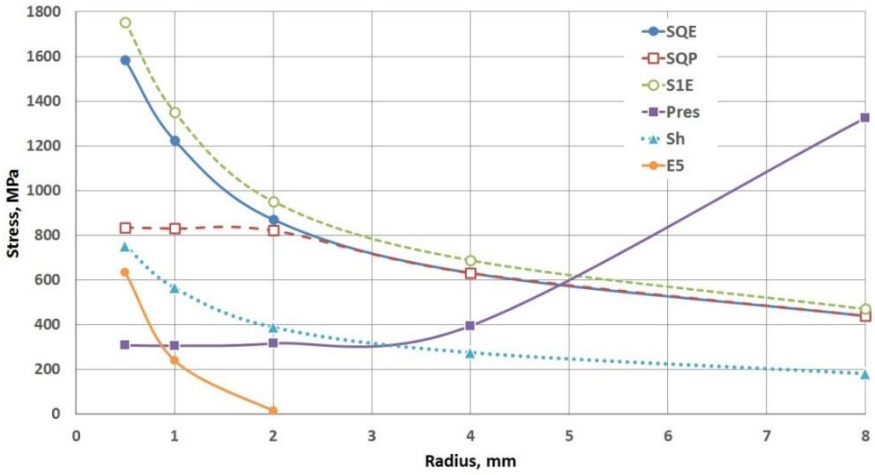

Fig. 10. Stress parameters (see above) and accumulated plastic deformation E5 on the pin fillet depending on radius

Centrifuge simulations (FC) were provided for the range of pin fillet radiuses. Results are collected in the tab. 1. Related graphs are showed on the fig. 10. Here designation *SQE* relates with fully elastic FEM-solution (EL). It is maximal equivalent stress on the pin fillet. Designation *S1E* discloses peak value of maximal principal stress σ_1 just here.

Table 1 – Stresses and plastic deformation on the pin fillet depending on radius produced

Design variant	*Des0*	*Des1*	*Des2*	*Des4*	*Des8*
Fillet radius r_f, mm	0.5	1	2	4	8
SQE (MPa)	1584	1225	870	631	439
SQP (MPa)	835	830	821	631	439
S1E (MPa)	1754	1351	951	688	470
Pres (MPa)	308	306	316	395	1325
Sh (MPa)	752	565	389	275	181
E5 (%, 10^{-3})	634	240	14.8	0	0

Designation SQP refers to equivalent stress σ_e distribution, revealed after elastic-plastic (PL) solution. Stress σ_e is limited here from above by yield stress of steel. It is accompanied by plastic deformation ε_{pl}^{ac} accumulation on the fillet surfaces (parameter E5 scaled in 10^5 times). Designation *Sh* describes hydrostatic stress. Large *Sh* value points out volume tension state. It is dangerous for brittle fracture initiation. Designation *Pres* is the maximal contact pressure at the ***CI-1*** ("pin – bucket") interface. Structural stresses (by curves *SQE*, *SQP*, *S1E*, *Sh* on fig. 10) relatively rapidly go down as fillet radius increases from 0.5 to 4 mm. Stress decreasing decelerates after level $r_f = 4$ mm passing by. Plastic deformations (*E5*) are revealed at the fillet only for $r_f = 2$ mm and lower.

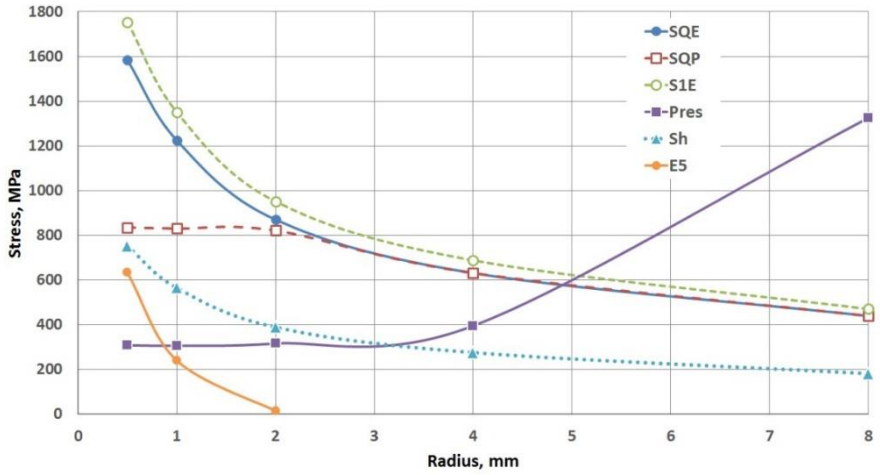

Fig. 10. Stress parameters (see above) and accumulated plastic deformation E5 on the pin fillet depending on radius

Contact pressure (*Pres*) begins to increase for $r_f = 4$ mm and higher. Thus fig. 10 analysis points out radius $r_f = 4$ mm (***Des4***) as optimal design solution for presented materials. Here structural stresses as contact ones are limited at the same time. Implementation of the *Des8* variant ($r_f = 8$ mm) needs to improve bucket slot durability due to high contact stresses. Laser treatment may be fulfilled for centrifuge safety accomplishing.

Conclusions. 1. Set of critical surviving points (CSP) is revealed in the centrifuge load-bearing system (LBS). They are placed at the pin fillets.

2. Hardened steel undergoes localized plastic deformation in the CSP on the pin fillets. However pins preserve strength as long-year exploit practice prove. Such kind of surviving needs special investigation. It may be due to autofrettage effect.

3. It is proposed to smooth out (blur, smear) pin CSP by fillet radius increasing. Stress concentrator smoothing is possible. Hence, in the limited design room it brings the contact pressure growing caused by contact spot shrinkage.

4. Pin fillet radius $r_f = 4$ mm is the optimal one. Equivalent stress is lowered in 1.94 times in comparison with $r_f = 1$ mm with no significant contact pressure increasing (29 % only). Simultaneously, hydrostatic pressure is declined in 2.05 times. It improves pin fillet protection from the brittle fracture.

5. Rising of the pin fillet radius is rather moderate instrument to decrease stress concentration. 8-times radius increasing lowers the tension stresses in 2.78 times only.

6. Contact spot control (CSC) demands precise finishing provided by 5-axis machine tools with grinding tooling. Conjunction of grinding and 5-axis machines points out to the new branch.

7. Fillet radius enlargement smooth the pin profile out. It is the step to the bionic design.

REFERENCES

1. Harrison, R. G. Bioseparations / R. G. Harrison [et al.] // Science and Engineering. Oxford University Press. – 2003.

2. Zienkiewicz, O. C. The finite element method / O. C. Zienkiewicz, R. L. Taylor // Basis. Oxford: Butterworth-Heinemann. – 2000. – Vol. 1.

3. Vasilevich, Yu. V., Finite element analysis of centreless-lunette turning of heavy shaft / Yu. V. Vasilevich, S. S. Dounar // Science & Technique. – 2017. – Vol. 16(3). – P. 196–205.

4. Vasilevich, Yu. V. finite element analysis of concrete filler influence on dynamic rigidity of heavy machine tool portal / Yu. V. Vasilevich, S. S. Dounar, I. A. Karabaniuk // Science & Technique. – 2016. – Vol. 15(3). – P. 233–241.

5. Dounar, S., Finite Element Method analysis of the deformation of the shaft and supports of the large, precise lathe – Cutting force excitation / S. Dounar, A. Iakimovitch, A. Jakubowski // Scientific Journals of the Maritime University of Szczecin. – 2020. – Vol. 62(134). – P. 91–98.

6. Rickwood, D. Biological Centrifugation / D. Rickwood, J. M. Graham // Springer Verlag; ISBN:0387915761. – 2001.

7. Yong, Z. 3 Parametric Nonlinear Finite Element Analysis of Strain Ratcheting in Pressurized Elbows Based on Random Vibration / Z. Yong, J. D. Stevenson, H. T. Tang // Shock and Vibration. – 1996. – Volume 3. – Article ID 978073.

8. Konig, J. A. Shakedown of Elastic-Plastic Structures / J. A. Konig // Elsevier. – 1987.

9. Dixit, U. Autofrettage Processes / U. Dixit, S. Kamal, R. Shufen // Boca Raton: CRC Press. – 2020.

10. Lu, K. Making stronger materials ductile with gradients / K. Lu // Science. – 2014. – Vol. 345, No. 6203. – P. 1455–1456.

11. Suresh, S. Fundamentals of Functionally Graded Materials / S. Suresh, A. Mortensen // IOM3, Maney Publishing. – London, UK. – 1998.

12. Ho, H. S. Shot Peening Effects on Subsurface Layer Properties and Fatigue Performance of Case-Hardened 18CrNiMo7-6 Steel / H. S. Ho [et al.] // Advances in Materials Science and Engineering. – 2018. – P. 11.

13. Lv, Y. Influence of different combined severe shot peening and laser surface melting treatments on the fatigue performance of 20CrMnTi steel gear / Y. Lv, L. Q. Lei, L. N. Sun // Materials Science and Engineering A. – 2016. – Vol. 658, P. 77–85.

Поступила: 19.01.2021